The Radiated Energy of the 2004 Sumatra-Andaman Earthquake

Hiroo Kanamaori

Seismological Laboratory, California Institute of Technology, Pasadena, California, USA

We use several independent methods to estimate the radiated energy E_R of the Sumatra-Andaman earthquake (M_w=9.0 to 9.3), and investigate whether the difference in the rupture patterns between north and south is reflected in the difference in the energy budget. First, we used a finite source model and estimated E_R to be 1.38x10^{17} J for a frequency band f (frequency) ≤ 0.1 Hz. Since this method is relatively free from many assumptions commonly made in energy estimation, this value is considered robust. To estimate E_R for a frequency band 0.1 < f ≤ 1 Hz, we used a frequency-domain analysis and obtained E_R =1.6 x10^{17} J for this frequency band. This estimate is somewhat uncertain because of the energy attenuation during propagation and the effect of the near-source structure. We also estimated E_R relative to the 2001 Bhuj, India, earthquakes for which a reliable estimate of E_R has been obtained. The total E_R thus estimated is 3.0x10^{17} J. The energy-moment ratio, 0.46x10^{-5}, is slightly smaller than that for other large subduction-zone earthquakes. The radiation efficiency defined by $\eta_R = (2\mu/\Delta\tau)(E_R/M_0)$ (μ=rigidity, M_0=seismic moment, $\Delta\tau$=static stress drop) is 0.16 which is smaller than that of many large earthquakes, and is between the values of regular earthquakes and slow tsunami earthquakes. The values of η_R for the Nicobar segment, the Nicobar-Andaman segments combined, and the Sumatra segment are 0.053, 0.11, and 0.21, respectively, which suggests that the slip in the northern segments involves a large amount of energy dissipation associated with water-filled thick sediments.

1. INTRODUCTION

The December 26, 2004, Sumatra-Andaman earthquake (M_w=9.2) has been studied in great detail by several groups of investigators [e.g., Bilham et al., 2005; Ni et al., 2005; Lay et al., 2005; Ammon et al., 2005; Park et al., 2005; Stein and Okal, 2005; Ishii et al., 2005; Banerjee et al., 2005; Vigny et al., 2005; Tsai et al., 2005]. (M_w ranges from 9.0 to 9.3 in the literature, and we use 9.2 here as a representative value.) It is one of the largest megathrust earthquakes and is unique in many respects. For example: (1) The rupture length, about 1300 km, is extremely long, the longest ever recorded; (2) The coseismic slip distribution varies significantly with a long tail to the north; (3) Seismic data, field data, and geodetic data combined suggest that the slip has a significant slow component on time scales longer than 1 hour, with a larger slow component to the north [Bilham, 2005; Banerjee et al., 2005]; more recent studies, however, suggest that the aseismic component was not as large as initially thought [Vigny et al., 2005; Subarya et al., 2005]. Chlieh et al. [2006] showed that the slip distribution determined from the GPS data obtained soon after the earthquake is about 40% larger than seismic slip over the Nocobar Is. segment; (4) The northern half (north of 7° N) ruptured

Earthquakes: Radiated Energy and the Physics of Faulting
Geophysical Monograph Series 170

10.1029/170GM07

on a plate boundary where a relatively old oceanic plate is subducting at a very oblique angle; this feature is different from that of many other megathrust earthquakes.

So far, most of the studies are focused on the determination of seismic moment M_0, and space-time distribution of slip. To gain further insight on the unique character of this event, an additional source parameter, the radiated energy E_R, needs to be determined accurately. The static parameter, seismic moment M_0, and the dynamic parameter E_R together with additional information on the source dimension provide important information on the physics of earthquakes through a macroscopic analysis of the energy budget [e.g., Husseini, 1977]. Although accurate estimation of E_R is still difficult, this approach provides useful comparisons between subduction megathrust earthquakes, shallow crustal earthquakes, slow tsunami earthquakes, and deep earthquakes [Venkataraman and Kanamori, 2004b].

For the Sumatra-Andaman earthquake, despite its extreme complexity in the rupture process, several factors work to our advantage. First, high-quality teleseismic data with high signal-to-noise ratio are available. Second, several source rupture models have been determined in great detail, and can be used for straightforward energy estimation. Third, because of the very large size of the event, simple scaling relations suggest that most energy is contained in the relatively long-period (longer than 1 sec) waves, which are much less affected by the complex source and propagation effects than shorter period waves.

In this paper, we use several independent methods to estimate E_R of the Sumatra-Andaman earthquake, and investigate whether this earthquake is different from other large earthquakes and whether the difference in the rupture patterns and physics between north and south is reflected in the difference in the energy budget.

2. ENERGY ESTIMATE FROM THE FINITE RUPTURE MODEL

For the 2004 Sumatra-Andaman earthquake, source rupture models have been determined by several investigators by inversion of teleseismic P waves [Ammon et al., 2005]. Since the source duration of this earthquake is so long (~600 sec) that the Green's functions to be used for inversion must include not only the P phase but also other phases like PP and PPP, as well as very long-period energy like the W phase [Kanamori, 1993]. One of the models (Model III) presented in Ammon et al. [2005] uses Green's functions computed with normal-mode summation and includes all these phases, and is thus most appropriate for the present study. The Green's functions were computed for the Preliminary Reference Earth Model (PREM) [Dziewonski and Anderson, 1981]. The resulting source model is represented by 812 point sources and is given as a function of time and space [Chen Ji, written communication, 2005]. The temporal and spatial distributions are schematically shown by figures 5 and 6 of Ammon et al. [2005]. This rupture model has a centroid depth of 31 km and can explain not only the body- and surface-wave forms, but also the normal-mode amplitudes up to 1 hour [Park et al., 2005].

Given this rupture model, estimation of the radiated energy is straightforward, as was done by Venkataraman and Kanamori [2004a] for the 1999 Hector Mine earthquake and the 1999 Chi-Chi, Taiwan earthquake. Since all the propagation effects including those due to attenuation and near-source reflections have been removed in construction of the source model, we place the 812 point sources in PREM, let them radiate, compute the far-field displacement, and estimate the radiated energy by summing up the energy flux through a spherical surface at a large distance from the source. The only complication is that the medium is not homogeneous, but layered as given by PREM. We handle this problem as follows. For simplicity, we consider only S waves for explanation of the method. In the source region of PREM, the density and velocity vary from the lower-crustal values (ρ_c=2.90 g/cm^3, v_c=3.90 km/s) to the upper mantle values (ρ_M=3.38 g/cm^3, v_M =4.488 km/s). For a point source with a moment rate function $M_0(t)$ in a medium with density ρ and velocity v, the radiated energy is given by [e.g., Vassiliou and Kanamori, 1982]

$$E_R \propto \left(1/\rho v^5\right)\int_0^\infty \dot{M}_0^2(t)dt$$

Thus, if we put the source in a homogeneous medium with ρ_c and v_c, or ρ_M and v_M, then, the energy ratio is $(\rho_M v_M^5 / \rho_c v_c^5)$ =2.4. If we put the source in PREM, the energy estimate should be between the two cases. In our computation, for each point source at a depth where density is ρ_i and velocity is v_i, we modify the displacement amplitude by the acoustic impedance ratio $\left(\rho_i v_i / \rho_0 v_0\right)^{1/2}$ before computing the far-field amplitude where ρ_0 and v_0 are the density and velocity at the surface where the energy flux is measured. The energy estimate does not depend on the choice of ρ_0 and v_0, as is the case for a point source. In the actual computation, we included both P and S wave energies and estimated the energy by low-pass filtering the source model at a cut-off frequency of f_c. The radiated energy thus computed is shown in Figure 1 as a function of f_c. Because of the limited frequency band used in inversion, the source model has little energy at frequencies above 0.1 Hz, as shown in Figure 1. The radiated energy thus estimated is E_R=1.38x10^{17} J for f_c=0.1 Hz. This value is 1.43 and 0.70 times of the energy estimated if the source is put in a homogeneous medium with (ρ_M=3.38 g/cm^3, v_M=4.488 km/s) and (ρ_c=2.90 g/cm^3, v_c=3.90 km/s), respectively, and is reasonable for E_R estimated for a source in PREM.

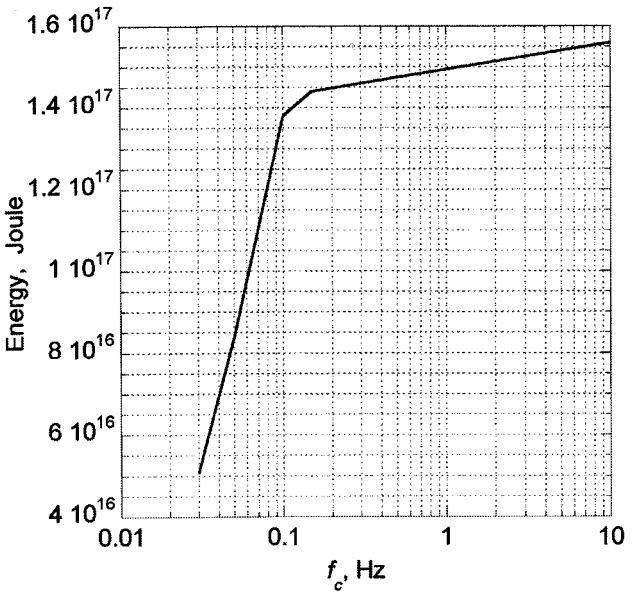

Figure 1. Radiated energy E_R estimated from the finite source rupture model (Model III in Ammon et al. [2005]) as a function of the cut-off frequency f_c.

Since no energy at frequencies higher than 0.1 Hz is included in this estimate, this is the lower bound of E_R of the 2004 Sumatra-Andaman earthquake. This method does not involve many assumptions, and E_R estimated this way can be regarded as a fairly robust lower bound as long as the source model is accurate.

3. FREQUENCY-DOMAIN ESTIMATES

We now estimate the energy contained in the frequency band higher than 0.1 Hz. The most widely used method for energy estimation is the one developed by Boatwright and Choy [1986]. Here we used a similar method used in Venkataraman and Kanamori [2004a] in which single station estimates of P-wave energy given by

$$E_\alpha = \frac{32\pi\rho_h\alpha_h R_E^2}{15C_{st}^2F_p^2g^2}\int_0^\infty |\dot{\hat{u}}_{p,st}(f)|^2 \exp(2\pi f t^*)df$$

are first computed for many stations distributed over a wide azimuthal range, and averaged. In the above, $\dot{\hat{u}}_{p,st}(f)$ is the frequency spectrum of the vertical component of ground-motion velocity at a station, and ρ_h, α_h, R_E, C_{st}, F_p, g, and t^* are the density at the source, P-wave velocity at the source, the radius of the Earth, the station amplification factor (the ratio of the vertical component of displacement to the amplitude of the incoming wave), the effective P-wave radiation pattern including the effect of near-source reflections such as pP and sP, the geometrical spreading factor, and the attenuation factor (travel time divided by the path average of quality factor Q). The integration is with frequency f. This expression, or the one similar to it, has been used to estimate the P-wave energy from teleseismic P waves. For the Sumatra-Andaman earthquake, the source duration is nearly 600 sec [Ni et al., 2005; Lay et al., 2005; Ishii et al., 2005], we need to use the records from the stations of which the S-P time is longer than 600 sec. This requirement limits the use of stations to those with the epicentral distance $\Delta \geq 70°$. Also, surface reflections such as PP and PPP arrive during the duration of P wave. We will correct for this effect by comparing the energy estimate with that for the 2001 Bhuj India earthquake, as we will show later. For the attenuation parameter t^*, we use the most recent result for subduction-zone earthquakes obtained by Perez-Campos et al. [2003]. We used 13 stations with $\Delta > 70°$, and used the P-wave record with a duration of 580 sec after the P arrival. We corrected the displacement spectra for attenuation using the frequency dependent t^* given by Perez-Campos et al. [2003]. Figure 2 shows the moment rate spectra estimated from the displacement spectra. In contrast to the estimate from the source rupture model, the spectrum at frequencies lower than 0.1 Hz is not reliable because the direct phase and the near-source reflections pP and sP interact coherently at periods comparable to the travel time differences, pP-P time and sP-P time, and the basic assumption (i.e., random phase) used for computing the effective radiation pattern F_p breaks down. At frequencies higher than 0.2 Hz, the spectral shape exhibits a regular decay with frequency approximately as f^{-2}.

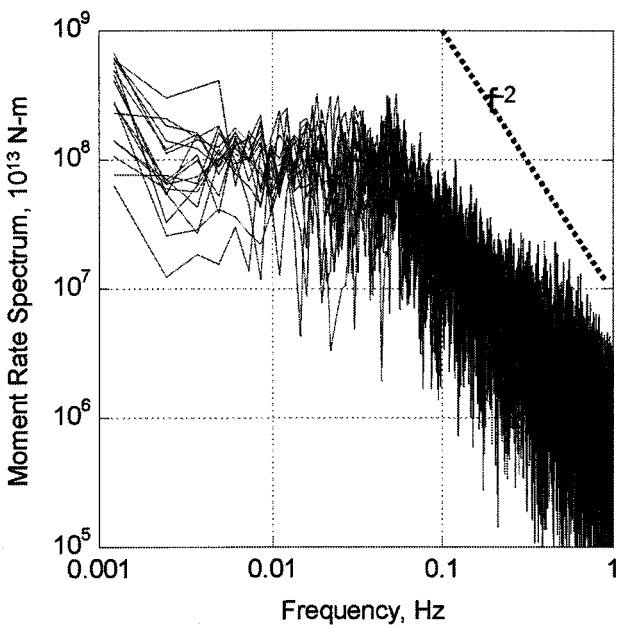

Figure 2. Moment rate spectra computed from the displacement records at 13 teleseismic stations.

We excluded the nodal stations for which F_p<0.7, because at these nodal stations small amount of the scattered energy can substantially affect the energy estimates. For this calculation, we used a mechanism given by (dip=14°, rake=110°, and strike=329°), placed the source at a depth of 20 km, and used ρ_h=2.87 g/cm^3 and α_h=6.5 km/s.

After the P-wave energy E_α has been estimated, it is multiplied by a factor

$$\left(\frac{3}{2}\right)\left(\frac{\alpha}{\beta}\right)^5$$

to estimate the S-wave energy E_β. Then the sum of E_α and E_β gives the total radiated energy E_R. Figure 3 shows azimuthally averaged E_R as a function of f_c which is the cut-off frequency at the high-frequency end. At this stage, the contributions from PP and PPP are included in the estimates, which need to be subtracted later.

Figure 4 shows the azimuthal distribution of E_R. No obvious directivity effect is observed. This is not surprising because, as shown by Venkataraman and Kanamori [2004a], the P-wave directivity effect is not very large for dip-slip earthquakes, and the simple azimuthal average yields a good estimate of the total energy radiation. Also, at the period range considered, the rupture speed could be somewhat irregular and prevents development of a coherent directivity pattern.

Many assumptions are made in this calculation, especially those on (1) t^*, (2) F_p, and , (3) point source depth. The estimate for f_c=0.1 Hz, 1.2x10^{17}J, is somewhat smaller than that estimated using the finite source model, E_R=1.38x10^{17} J, especially if we divide it by 1.34 to correct for the effect of PP etc, as we will discuss later. However, this difference is what is expected because at low frequencies, P and pP and P and sP tend to destructively interfere each other resulting in smaller

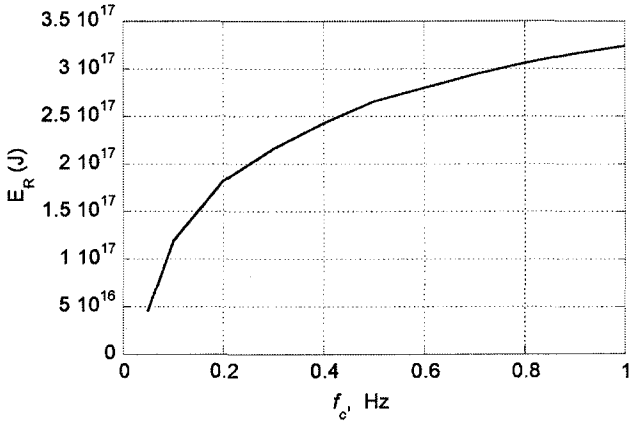

Figure 3. The radiated energy E_R as a function of high-cut frequency f_c.

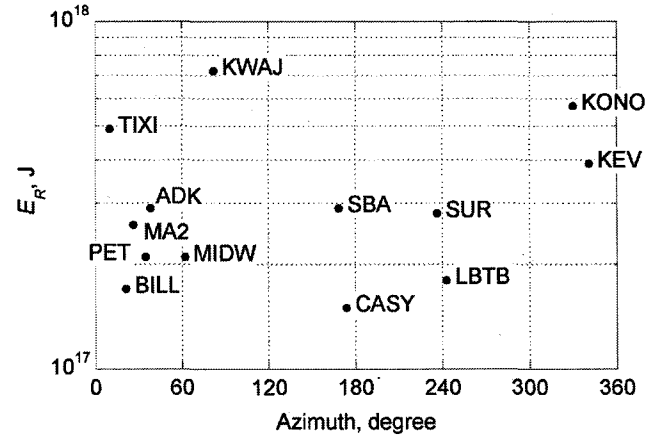

Figure 4. Azimuthal variation of E_R.

amplitude at teleseismic distances. In any case, we will not use the estimate at frequencies lower than 0.1 Hz.

The energy contained in the frequency range between 0.1 to 1 Hz, is 2.1x10^{17} J. This includes the contributions from PP, PPP etc, which must be subtracted. Although we could not determine the energy spectrum at frequencies higher than 1 Hz, if the approximate f^{-2} trend seen in Figure 2 continues to higher frequencies, the error in energy estimates caused by truncation of integration at 1 Hz is less than 3 %.

4. COMPARISON WITH THE 2001 BHUJ EARTHQUAKE (M_w=7.6) AND REMOVAL OF THE CONTRIBUTIONS OF PP, PPP AND OTHER SCATTERED ENERGIES

Figure 5 shows typical examples (station TIXI) of the P-wave records of the Sumatra-Andaman earthquake, the 2001 Bhuj, India, earthquake (M_w=7.6) and the 2005 Nias, Sumatra, earthquake (M_w =8.6). This figure is useful for getting the overall picture of the difference in energy radiation among these three earthquakes. The seismograms are plotted with the same scale, both in time and amplitude. The radiated energy of the Bhuj earthquake has been determined from various types of data [Singh et al., 2004; Venkataraman and Kanamori, 2004b] and the estimates of E_R obtained with different methods are in good agreement ranging from 1.9 to 2.1x10^{16} J. We take E_R=2x10^{16} J as a representative value for this earthquake. We can use the Bhuj earthquake as a calibration event, and estimate E_R of the Sumatra-Andaman earthquake with respect to it.

The P-wave pulse of the Bhuj earthquake is impulsive with a duration of about 40 sec. After the P pulse, PP and PPP and other scattered energies are seen. The gray curve is the integral of velocity-squared which is proportional to the radiated energy. The initial part of the dashed curve

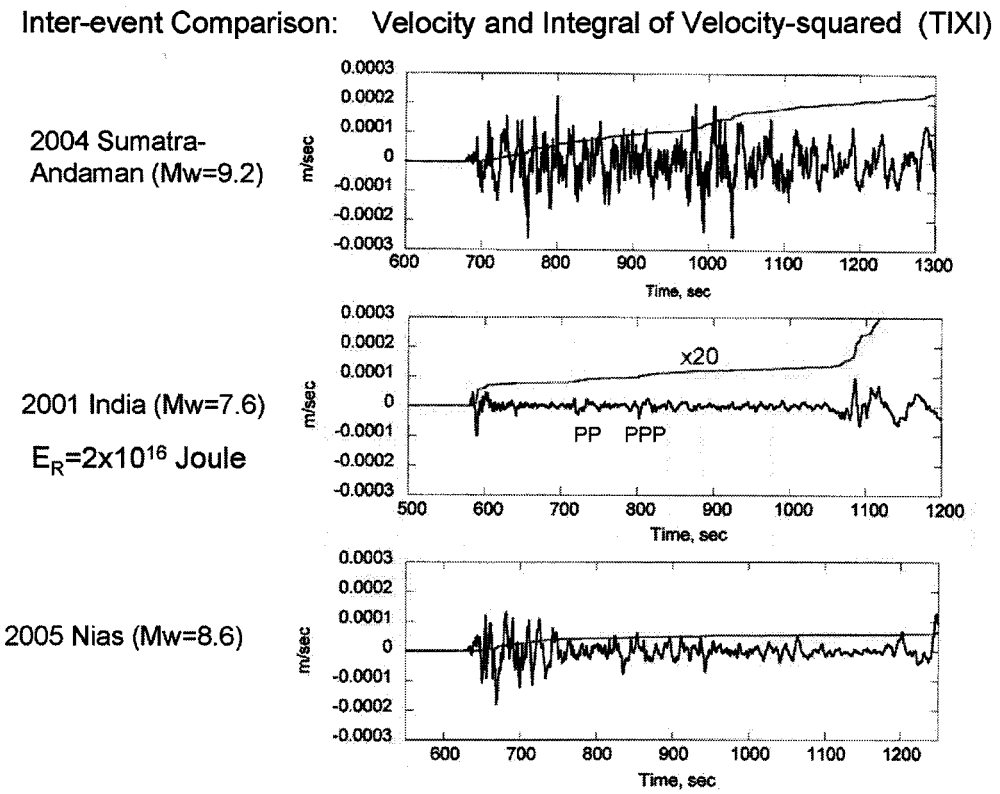

Figure 5. Comparison of the 2004 Sumatra-Andaman, 2001 Bhuj, India, and 2005 Nias, Sumatra earthquakes. The velocity record (dark curve) and the integral of velocity-squared (gray curve) are shown. The integral of the velocity-squared for the Bhuj earthquake is multiplied by a factor of 20 for comparison with other events.

to about 100 sec after the P arrival represents the radiated energy from this event, and the following gradual increase represents the contribution of PP, PPP and other scattered energies. In contrast, the P-wave record of the Sumatra-Andaman earthquake is extremely complex reflecting the long duration of the rupture process of this earthquake. The integral of the velocity-squared keeps increasing as a result of continuous energy radiation from the source. The effect of PP, PPP and other scattered energies is embedded in the complex waveform and is not evident, but it is included in the integral. For comparison, the integral of the velocity-squared for the Bhuj earthquake is multiplied by 20 with respect to that for the Sumatra-Andaman earthquake. This comparison suggests that E_R of the Sumatra-Andaman earthquake is at least an order of magnitude larger than that of the Bhuj earthquake. Figure 5 includes a similar plot for the 2005 Nias, Sumatra, earthquake (M_w=8.6) for comparison. Since the mechanism and depth of these earthquakes are different, we need to make a more detailed analysis for quantitative comparison.

We performed the same analysis as described in section **3** for the Sumatra-Andaman earthquake for the Bhuj, and Nias earthquakes, while varying the duration of the records used. The result is shown in Figure 6. We used 18 and 7 stations for the Bhuj, and Nias earthquakes respectively, with $\Delta \geq 70°$ and $F_p > 0.7$.

Now we subtract the contributions of PP, PPP, and other scattered energies. Since the duration of P-wave for the Bhuj earthquake is less than 70 sec, as shown in Figure 5, the energy estimate using the record with a duration of 80 sec should yield the correct estimate of E_R. If we extend the records to 580 sec, the same as that used for the Sumatra-Andaman earthquake, the estimate includes the effect of PP and PPP etc. Thus, the ratio of E_R(580 s)/E_R(80 s) should give the approximate effect of PP and other phases. From Figure 6, the ratio is E_R(580 s)/E_R(80 s) =1.5. Then, to correct for the effect of PP etc on the E_R estimate of the Sumatra-Andaman earthquake, we divide E_R obtained in section **3** above by a factor similar to this. Actually, for the later part of the energy radiation, PP and other scattered energies arrive after the time window of the integration, and the factor should be smaller than 1.5. Correcting for this effect, we find that the appropriate factor is 1.34. Thus, E_R (0.1Hz<f<1.0Hz)=2.1/1.34=1.57 x 10^{17} J for the Sumatra-Andaman earthquake.

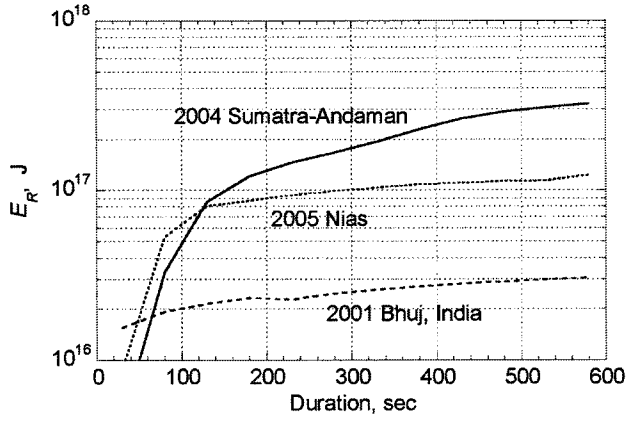

Figure 6. The radiated energy E_R as a function of record length after the P-wave arrival.

In more detail, the contribution of the later phases is slightly frequency dependent. The correction factor is 1.67, 1.35, and 1.23 for the frequency bands of 0.10-0.25 Hz, 0.25-0.50 Hz, and 0.50-1.0 Hz, respectively, and if we apply this correction separately to E_R contained in each frequency band, the total E_R for the frequency band from 0.1 to 1 Hz is 1.60×10^{17} J.

In this method, we did not use the absolute value of E_R for the Bhuj earthquake; only the energy ratio of different time intervals is used for removing the effect of PP etc. Next, we use the absolute value E_R of the Bhuj earthquake, and estimate E_R of the Sumatra-Andaman earthquake with respect to it. From Figure 6, the E_R ratio of the Sumatra-Andaman to the Bhuj earthquakes is 10.6 when measured with the total duration of 580 sec. If we correct for the effect of PP and other scattered energies, the actual energy ratio must be 10.6(1.50/1.34)=11.9 using the correction factors determined above. Since E_R of the Bhuj earthquake is 2×10^{16} J, we estimate that E_R of the Sumatra-Andaman earthquake is 2.4×10^{17} J.

5. SUMMARY OF ENERGY ESTIMATES

The estimates of the radiated energy of the 2004 Sumatra-Andaman earthquake described above can be summarized as follows.

E_R for $f_c \leq 0.1$ HZ from the finite source model	1.38×10^{17} J
E_R from the velocity spectrum 0.1Hz $< f <$ 1 Hz after the contributions of P, PP and scattered energies have been removed	1.60×10^{17} J
Total	2.98×10^{17} J
E_R relative to the 2001 Bhuj earthquake (E_R=2×10^{16} J)	2.4×10^{17} J

Although the estimate of E_R is still subject to considerable uncertainty due to several factors, especially the source structure, t^*, and the contribution from the frequency band higher than 1 Hz, the lower bound estimated from the finite source model is considered robust. Also, the inter-event comparison with the 2001 Bhuj earthquake provides a useful check, because E_R of the Bhuj earthquake is considered fairly reliable because of the availability of both regional and teleseismic data and of the relatively simple source process as shown in Figure 5. In view of the robustness of the estimate from the finite source model, and the uncertainties arising from the interference of P and pP and P and sP at low frequencies, we prefer the estimate E_R=3.0×10^{17} J (the 3rd row of the table above, rounded to 2 digit). The overall consistency of the E_R estimates from the finite source model, the velocity spectrum, and the inter-event comparison gives confidence to this value.

The value of E_R obtained here is larger than that listed in the U.S.G.S. web site http://neic.usgs.gov/neis/eqlists/sig_2004.html), 1.1×10^{17} J, and smaller than that listed in Lay et al. [2005], 1.1×10^{18} J. Many factors contribute to this difference, and the spread of this magnitude is common with preliminary energy determinations.

The large estimate in Lay et al. [2005] is mainly a result of the following: (1)A constant t^*=1 sec is used. (2) A minimum F_p factor of 0.3 is used. (3) The HVD CMT mechanism (dip=8°, rake=110°, strike=329°) is used. A combination of these factors increases the estimate of the energy by a factor of 2 to 3 compared with that obtained in this study. Other differences in the choice of stations, the source velocity structure etc contributed to the larger estimate in Lay et al.[2005]. The low estimate of the preliminary USGS result is partially due to the too short time window used for energy integration. The more recent study by Choy and Boatwright [2006] corrected this problem and their estimate has increased to 1.3×10^{17} J. This is still about a factor of 2 smaller than the estimate in this paper. The phase-coherent interaction between P and sP at the source tends to reduce the amplitude, which could be responsible for their smaller estimate. Considering all the uncertainties, it appears that the factor of 2 agreement is satisfactory.

6. ENERGY-MOMENT RATIO AND THE RADIATION EFFICIENCY

The ratio of the radiated energy to seismic moment (scaled energy), $\tilde{e} = E_R / M_0$, is a useful macroscopic parameter to characterize the overall dynamic property of an earthquake [e.g., Kanamori et al., 1993]. This ratio multiplied by rigidity is called the apparent stress and has long been used in seismology [Aki, 1966; Wyss and Brune, 1968]. Since $\tilde{e}=E_R / M_0 = (1/\mu)(1/D)(E_R / A)$ (D=fault slip, A=fault area),

it is proportional to the energy radiation scaled by the fault area and slip. This parameter can be determined solely from the two macroscopic parameters E_R and M_0 without making further assumptions on the source dimension.

The seismic moment of the Sumatra-Andaman earthquake has been determined by several investigators [e.g., Stein and Okal, 2005; Ammon et al., 2005; Park et al., 2005; Tsai et al., 2005]. Excluding the contribution from the slow slip estimated from the GPS data, it ranges from 6 to11 x10^{22} N-m. The difference is mainly due to the different choice of the depth and dip angle by different investigators, and until source inversion using a realistic 3-dimensional source structure is performed, the difference is not meaningful. Here, for consistency's sake, we use M_0=6.5x10^{22} N-m given by the finite-fault model used in this study (Model III in Ammon et al. [2005]). Note that, this value is for the rapid co-seismic slip (a local time scale of 50 sec with a total rupture time of about 550 sec) , and does not include the slow transient and post seismic slip on time scales longer than 1 hour. Then we obtain for the Sumatra-Andaman earthquake as a whole, $\tilde{e} = E_R / M_0$=4.6x10^{-6}. This value can be compared with the results for subduction-zone earthquakes determined and compiled by Bilek et al.[2004]. The value for the Sumatra-Andaman earthquake is similar to those of large dip-slip earthquakes determined by Kikuchi and Fukao [1988] and Bilek et al.[2004], but is smaller than those determined by Choy and Boatwright [1995], Newman and Okal [1998], Perez-Campos et al. [2003] and Venkataraman and Kanamori [2004b]. For comparison, the ratio for the 2001 Bhuj earthquake, 6.2x10^{-5} [Singh et al, 2004], is about an order of magnitude larger. For further comparison, we estimated E_R for two recent subduction-zone earthquakes, 2001 Peruvian earthquake (M_w=8.4) and the 2003 Tokachi Oki earthquake (M_w=8.3). The values of E_R and the ratio $\tilde{e}$ are listed in Table 1; the values of $\tilde{e}$ are similar to that of the Sumatra-Andaman earthquake. Thus, the ratio $\tilde{e}$ for the Sumatra-Andaman earthquake is not particularly anomalous, and is slightly on the low side.

The rupture zone of the Sumatra-Andaman earthquake can be divided into three segments, Sumatra, Nicobar and Andaman segments, as shown by figure 8 of Lay et al. [2005]. From the spatial and temporal variations of the moment given by Model III in Ammon et al. [2005], and the temporal variation of E_R shown in Figure 7, we can estimate $\tilde{e}$ separately for each segment with the assumption that the 3 segments do not interact in energy radiation. The E_R curve shown in Figure 7 is constructed by combining E_R estimated from the finite fault model for the frequency band from 0 to 0.1 Hz, and E_R estimated for the frequency band from 0.1 to 1 Hz,with the frequency-domain analysis after the contributions of PP etc have been removed. Since the estimate of M_0 for the Andaman segment is from the tail end of the moment rate function and is not reliable, we did not compute $\tilde{e}$ for this segment. The results are listed in Table 1. Although the energy-moment ratio, $\tilde{e}$, is a useful dynamic parameter, $\tilde{e}$ itself does not completely reflect the difference in the rupture physics in terms of the energy budget. The radiation efficiency η_R is more representative of the rupture physics.

The radiation efficiency was introduced by Husseini [1977] and recently used by Venkataraman and Kanamori [2004b] for characterizing the dynamic behavior of large earthquakes. A difficulty in going from $\tilde{e}$ to η_R is the difficulty in estimating the average static stress drop, $\Delta\tau$. The stress drop varies spatially on the fault plane, and some ambiguity is inevitable in estimating $\Delta\tau$, especially for a very complex event like the Sumatra-Andaman earthquake. For this earthquake, we can use the relation for a long dip-slip earthquake, $\Delta\tau = c\mu D / W$ where D is the average slip, W is the average width, and c is the geometrical factor given by $c = 4(\lambda+\mu) / \pi(\lambda+2\mu)$ or $c = 8(\lambda+\mu) / \pi(\lambda+2\mu)$ depending on whether the slip breaks the surface or not [Boore and Dunbar, 1977]. For the Sumatra-Andaman earthquake, slip decreases at shallow depth with most of the slip at depths. Thus, we use the case for a buried fault. We use the fault length L and width W for the three segments from figure 8 of Lay et al., [2005]. For the estimates of W we used the

Table 1. Source Parameters of the Sumatra-Andaman Earthquake and Other Large Earthquakes.

Event or Segment	L (km)	W(km)	M_0 (10^{21} N-m)	D (m)	$\Delta\tau$ (MP)	E_R (10^{17}J)	$\tilde{e}=E_R/M_0$ (10^{-5})	η_R
Andaman	570	120	13	2.8	2.7	0.60		
Nicobar	325	128	22	7.8	7.0	0.60	0.27	0.053
Sumatra	420	180	30	5.8	3.8	1.7	0.57	0.21
Sumatra-Andaman, Total	1315	141	65	4.9	3.8	3.0	0.46	0.16
Nias	300	110	11	4.9	5.2	0.82	0.75	0.20
2001 Bhuj			0.31			0.21	6.2	0.23
2001 Peru			4.7			0.33	0.70	
2003 Tokachi-Oki			3.10			0.20	0.65	

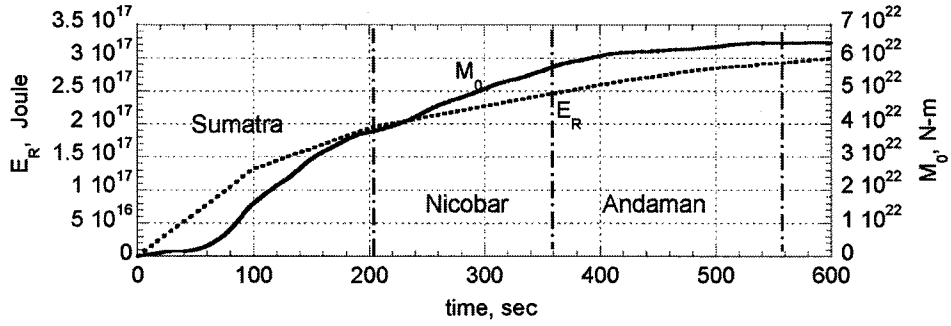

Figure 7. Temporal variation of M_0 (solid curve) and E_R (dotted curve) for the 2004 Sumatra-Andaman earthquake. Vertical dash-dot lines separate the Sumatra, Nicobar, and Andaman segments.

values which is 75% of the width of the boxes in Lay et al. [2005] to represent the effective width. This reduced width is consistent with that inferred from the slip distribution shown in Ammon et al. [2005]

Although the interpretation of η_R is model dependent, if we use the widely used breakdown-zone interpretation of the slip weakening model [Li, 1987], it is defined by the ratio of E_R to the potential energy available for strain release (i.e., total potential energy change minus the energy loss due to slip under constant friction [Rice, 1980]), $\Delta E_{T0} = (1/2)\Delta\tau DA$, and is given by

$$\eta_R = E_R / \Delta E_{T0} = (2\mu/\Delta\tau)(E_R / M_0)$$

The values of η_R thus determined are listed in Table 1, and shown in Figure 8.

7. DISCUSSION AND CONCLUSIONS

Since the finite source model we used can explain a large body of seismic data from body waves, surface waves, to normal mode, the estimate of E_R obtained from it is considered reliable over the frequency band lower than 0.1 Hz. The estimate of E_R contained over the frequency band from 0.1 to 1 Hz is somewhat uncertain because of the energy attenuation during propagation and the effect of the near-source structure. Nevertheless, the comparison of the direct frequency-domain estimate with that of the 2001 Bhuj, India, earthquake suggests that the value E_R =1.57x10^{17} J ($0.1 < f \leq 1.0$ Hz) is reasonable.

The energy-moment ratio (scaled energy) $\tilde{e} = E_R / M_0$ =0.46x10^{-5} is considerably smaller than that of many large earthquakes compiled by Venkataraman and Kanamori [2004b] and Perez-Campos et al. [2003]. However, it is still within the range for large subduction-zone earthquakes. Table 1 suggests that the radiation efficiency, η_R, for the Nicobar segment, is approximately 1/4 of that of the southernmost Sumatra segment, suggesting that the slip in the Nicobar segment involved a more energy dissipating process. Although we did not compute η_R for the Andaman segment itself because of the large uncertainty in M_0 for this segment, η_R for the Nicobar and Andaman segments combined is 0.11 and is about ½ of that of the southernmost Sumatra segment. The absolute values of η_R depend on the estimate of $\Delta\tau$ which is subject to large uncertainty, but the relative values are considered more robust.

The values of η_R for the Nicobar segment approaches those of the tsunami earthquakes such as the 1992 Nicaragua earthquake, the 1996 Peruvian earthquake, and the 1994 Java earthquakes listed by Venkataraman and Kanamori [2004b]. Venkataraman and Kanamori [2004b] attributed the energy dissipation to volumetric deformation of the water-filled sediments on the subduction boundary. A similar mechanism may be responsible for the energy dissipation in the northern segments. The thickness of the sediments along the trench

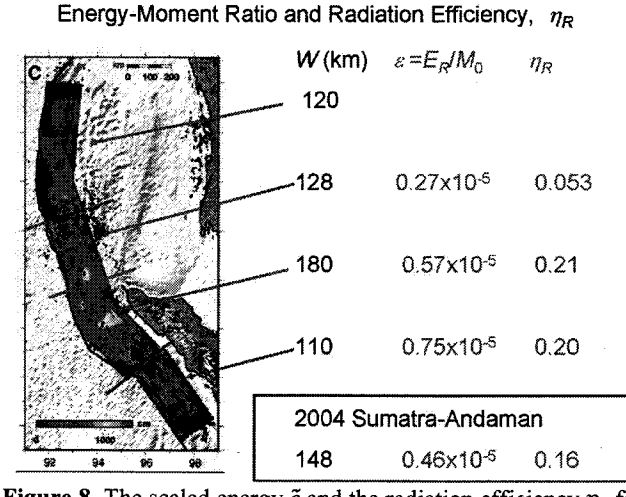

Figure 8. The scaled energy $\tilde{e}$ and the radiation efficiency η_R for the 2004 Sumatra-Andaman earthquake, the 2005 Nias earthquake, and the two segments (Sumatra and Nicobar segments) of the Sumatra-Andaman earthquake.

increases gradually from 1 km to more than 4km going from Sumatra to the northern Andaman Is.

In general, the radiation efficiency η_R can be related to the rupture speed [Husseini and Randall, 1976]. If the energy dissipation near the fault tip during rupture propagation is large, the rupture speed, V_R, decreases. Theories by Mott [1948], Kostrov [1966], Eshelby[1969], Freund [1972], and Fossum and Freund [1976] suggest that,

$$\eta_R \approx (V_R / \beta)^{1 \text{ to } 2}$$

where β is the shear-wave speed. Although this should be regarded as a very approximate relation, it provides a useful means for relating η_R to V_R. For most large earthquakes (V_R/β) > 0.5 (e.g., Venkataraman and Kanamori [2004b]), suggesting that η_R is larger than 0.25. The average rupture speed of the Sumatra-Andaman earthquake has been determined as 2.5 km/s from the directivity of teleseismic high-frequency wave [Ni et al., 2005] and as 2.8 km/sec from back-projection of the Japanese Hinet data [Ishii et al., 2005]. Tolstoy et al. [2005] investigated the T phase from this earthquake, and concluded that the rupture speed slowed down from 2.8 to 2.1 km/s at about 450 km northward from the epicenter, between the Sumatra and the Nicobar segments. Compared with the shear velocity, 3.74 km/s, in the lower crust where most of the slip occurred, these velocities are fairly low. The results obtained by de Groot-Hedlin [2005] and Guilbert et al. [2005] are qualitatively consistent with Tolstoy et al.'s [2005]. This transition is consistent with η_R being smaller for the Nicobar segment than for the Sumatra segment. Figure 9 shows the relationship between the rupture speed and η_R for the Sumatra segment, the Nicobar segment, and the Sumatra-Andaman earthquake as a whole. In general, η_R for the Sumatran-Andaman earthquake sequence is smaller than that for many large earthquakes, and is between slow tsunami earthquakes and the regular earthquakes.

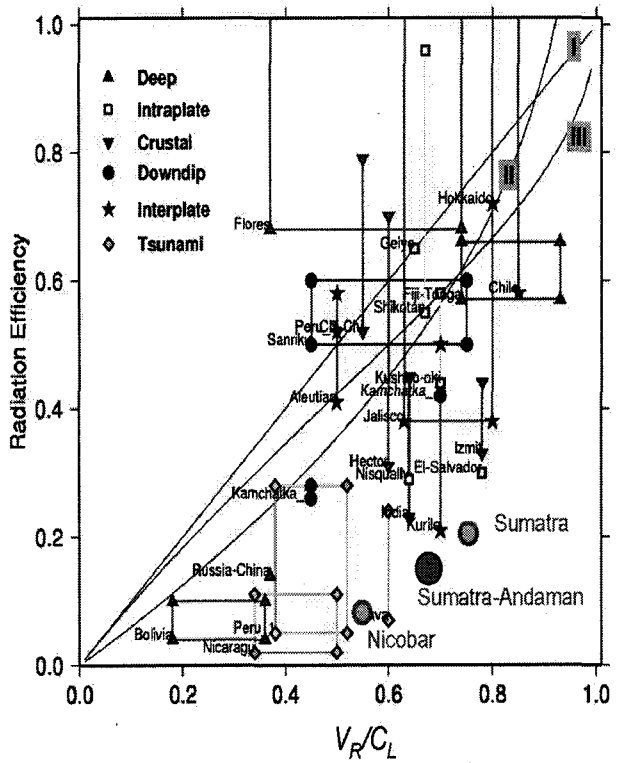

Figure 9. The relationship between the radiation efficiency and the rupture speed for the Sumatra segment, the Nicobar segment, and the Sumatra-Andaman earthquake as a whole. The base figure is taken from Venkataraman and Kanamori [2004b].

Acknowledgments. I thank Chen Ji for providing me with the details of the finite source model for the Sumatra-Andaman earthquake. I thank Luis Rivera, Krishna Singh, and Greg Beroza for thoughtful comments for improvement. The seismograms used for this study were provided by the Global Seismic Network of the Incorporated Research Institutions for Seismology.

REFERENCES

Aki, K. (1966), Generation and propagation of G waves from the Niigata earthquake ofJune 16, 1964. Part 2. Estimation of earthquake moment, from the G wave spectrum, *Bull. Earthquake Res. Inst. Tokyo Univ.*, *44*, 73–88.

Ammon, C. J., C. Ji, H. K. Thio, et al. (2005), Rupture process of the 2004 Sumatra-Andaman earthquake, *Science*, *308*, 1133–1139.

Banerjee, P., F. F. Pollitz, and R. Burgmann (2005), The size and duration of the Sumatra-Andaman earthquake from far-field static offsets, *Science*, *308*, 1769–1772.

Bilek, S. L., T. Lay, and L. J. Ruff (2004), Radiated seismic energy and earthquake source duration variations from teleseismic source time functions for shallow subduction zone thrust earthquakes, *Journal of Geophysical Research-Solid Earth*, *109*, B09308, doi:09310.01029/02004JB003039.

Bilham, R. (2005), A flying start, then a slow slip, *Science*, *308*, 1126–1127.

Boatwright, J., and G. L. Choy (1986), Teleseismic estimates of the energy radiated by shallow earthquakes, *J. Geophys. Res.*, *91*, 2095–2112.

Boore, D. M., and W. S. Dunbar (1977), Effect of Free-Surface on Calculated Stress Drops, *Bulletin of the Seismological Society of America*, *67*, 1661–1664.

Chlieh, M., J.-P. Avouac, V. Hjorleifsdottir, et al. (2006), Coseismic slip and afterslip of the great (Mw=9.15) Sumatra-Andaman earthquake of 2004, *Bull. Seismol. Soc. Am.*, in press.

Choy, G. L., and J. L. Boatwright (1995), Global patterns of radiated energy and apparent stress, *J. Geophys. Res.*, *100*, 18205–18228.

Choy, G. L., and J. L. Boatwright (2006), The energy radiated by the December 26, 2004 Sumatra-Andaman earthquake estimated from 10-minute P-wave windows, *Bull. Seismol. Soc. Am.*, *100*, in press.

de Groot-Hedlin, C. D. (2005), Estimation of the rupture length and velocity of the Great Sumatra earthquake of Dec 26, 2004 using hydroacoustic signals, *Geophysical Research Letters*, *32*, L11303, doi:11310.11029/12005GL022695.

Dziewonski, A. M., and D. L. Anderson (1981), Preliminary reference Earth model, *Phys. Planet. Inter.* , *25*, 297–356.

Eshelby, J. D. (1969), The elastic field of a crack extending non-uniformly under general anti-plane loading, *J. Mech. Phys. Solids*, *17*, 177–199.

Fossum, A. F., and L. B. Freund (1975), Nonuniformly Moving Shear Crack Model of a Shallow Focus Earthquake Mechanism, *J. Geophys. Res.*, *80*, 3343–3347.

Freund, L. B. (1972), Energy flux into the tip of an extending crack in an elastic solid, *J. Elasticity*, *2*, 341–349.

Guilbert, J., J. Vergoz, E. Schissele, A. Roueff, and Y. Cansi (2005), Use of hydroacoustic and seismic arrays to observe rupture propagation and source extent of the M-w=9.0 Sumatra earthquake, *Geophysical Research Letters*, *32*, L15310, doi:15310.11029/12005GL022966.

Husseini, M. I. (1977), Energy balance for formation along a fault, *Geophys. J. Roy. Astron. Soc.*, *49*, 699–714.

Husseini, M. I., and M. Randall (1976), Rupture velocity and radiation efficiency, *Bull. Seismol. Soc. Am.*, *66*, 1173–1187.

Ishii, M., P. M. Shearer, H. Houston, and J. E. Vidale (2005), Extent, duration and speed of the 2004 Sumatra-Andaman earthquake imaged by the Hi-Net array, *Nature*, *435*, 933–936.

Kanamori, H. (1993), W Phase, *Geophys. Res. Lett.*, *20*, 1691–1694.

Kanamori, H., J. Mori, E. Hauksson, T. H. Heaton, L. K. Hutton, and L. M. Jones (1993), Determination of Earthquake Energy-Release and M(L) Using Terrascope, *Bulletin of the Seismological Society of America*, *83*, 330–346.

Kikuchi, M., and Y. Fukao (1988), Seismic wave energy inferred from long-period body wave inversion, *Bull. Seismol. Soc. Am.*, *78*, 1707–1724.

Kostrov, B. V. (1966), Unsteady propagation of longitudinal shear cracks, *J. Appl. Math. Mech. (transl. P. M. M.)*, *30*, 1241–1248.

Lay, T., H. Kanamori, C. J. Ammon, et al. (2005), The great Sumatra-Andaman earthquake of 26 December 2004, *Science*, *308*, 1127–1133.

Li, V. C. (1987), Mechanics of shear rupture applied to earthquake zones, in *Fracture Mechanics of Rock*, edited, pp. 351–428, Acdemic Press, London.

Mott, N. F. (1948), Brittle fracture in mild steel plates, *Engineering*, *165*, 16.

Newman, A. V., and E. A. Okal (1998), Teleseismic estimates of radiated seismic energy: The E/M-0 discriminant for tsunami earthquakes, *Journal of Geophysical Research-Solid Earth*, *103*, 26885–26898.

Ni, S., H. Kanamori, and D. Helmberger (2005), Seismology—Energy radiation from the Sumatra earthquake, *Nature*, *434*, 582–582.

Park, J., T. R. A. Song, J. Tromp, et al. (2005), Earth's free oscillations excited by the 26 December 2004 Sumatra-Andaman earthquake, *Science*, *308*, 1139–1144.

Perez-Campos, X., S. K. Singh, and G. C. Beroza (2003), Reconciling teleseismic and regional estimates of seismic energy, *Bulletin of the Seismological Society of America*, *93*, 2123–2130.

Rice, J. R. (1980), The mechanics of earthquake rupture, in *Physics of the Earth's Interior*, edited by A. M. D. a. E. Boschi, pp. 555–649, North-Holland, Amsterdam.

Singh, S. K., J. F. Pacheco, B. K. Bansal, X. Perez-Campos, R. S. Dattatrayam, and G. Suresh (2004), A source study of the Bhuj, India, earthquake of 26 January 2001 (M-w 7.6), *Bulletin of the Seismological Society of America*, *94*, 1195–1206.

Stein, S., and E. A. Okal (2005), Speed and size of the Sumatra earthquake, *Nature*, *434*, 581–582.

Subarya, C., M. Chlieh, L. Prawirodirdjo, J.-P. Avouac, Y. Bock, K. Sieh, A. J. Meltzner, D. H. Natawidjaja, and R. McCaffrey (2005), Plate-boundary deformation of the great Aceh-Andaman earthquake, *Nature, in press.*

Tolstoy, M., R. DelWayne, and R. Bohnenstiehl (2005), Hydroacoustic constraints on the rupture duration, length, and speed of the great Sumatra-Andaman earthquake, *Seismological Research Letters*, *76*, 419–425.

Tsai, V. C., M. Nettles, G. Ekstrom, and A. M. Dziewonski (2005), Multiple CMT source analysis of the 2004 Sumatra earthquake, *Geophysical Research Letters*, *32*, L17304, doi:17310.11029/12005GL023813.

Vassiliou, M. S., and H. Kanamori (1982), The energy release in earthquakes, *Bull. Seismol. Soc. Am.*, *72*, 371–387.

Venkataraman, A., and H. Kanamori (2004a), Effect of directivity on estimates of radiated seismic energy, *J. Geophys. Res.*, *109*, B04301, doi:04310.01029/02003JB002548.

Venkataraman, A., and H. Kanamori (2004b), Observational constraints on the fracture energy of subduction zone earthquakes, *J. Geophys. Res.*, *109*, B05302, doi:05310.01029/02003JB002549.

Venkataraman, A., L. Rivera, and H. Kanamori (2002), Radiated energy from the October 16, 1999 Hector Mine Earthquake: Regional and Teleseismic Estimates, *Bull. Seismol. Soc. Am.*, *92*, 1256–1265.

Vigny, C., W. J. F. Simons, S. Abu, et al. (2005), Insight into the 2004 Sumatra-Andaman earthquake from GPS measurements in southeast Asia, *Nature*, *436*, 201–206.

Wyss, M., and J. N. Brune (1968), Seismic Moment Stress and Source Dimensions for Earthquakes in California-Nevada Region, *Journal of Geophysical Research*, *73*, 4681–4694.